

## PROCESSING MAGNETIC FIELD DATA FROM TABLET COMPUTERS USING CLUSTERING ALGORITHMS

ALESSIA AMELIO<sup>1,\*</sup>, RADMILA JANKOVIĆ BABIĆ<sup>2</sup>, IVO R. DRAGANOV<sup>3</sup>  
AND MARIJANA ČOSOVIĆ<sup>4</sup>

<sup>1</sup>Department InGeo  
University “G. d’Annunzio” Chieti-Pescara  
Viale Pindaro 42, Pescara 65127, Italy  
\*Corresponding author: alessia.amelio@unich.it

<sup>2</sup>Department of Computer Science  
Mathematical Institute of the Serbian Academy of Sciences and Arts  
Kneza Mihaila 36, Beograd 11000, Serbia  
rjankovic@mi.sanu.ac.rs

<sup>3</sup>Faculty of Telecommunications  
Technical University of Sofia  
8 Kl. Ohridski Blvd, Sofia 1000, Bulgaria  
idraganov@tu-sofia.bg

<sup>4</sup>Faculty of Electrical Engineering  
University of East Sarajevo  
Vuka Karadžića 30, Lukavica 71123, Bosnia and Herzegovina  
marijana.cosovic@etf.ues.rs.ba

Received December 2022; accepted February 2023

**ABSTRACT.** *The purpose of this paper is to extend our previous approach for detecting magnetic field ranges emitted by laptops to the tablet computers. Accordingly, we introduce a new analysis of the extremely low frequency magnetic field emitted by tablets using clustering algorithms. In particular, we compare partition-based, model-based, hierarchical, and density-based algorithms for clustering magnetic field values measured at the top and bottom positions of the tablet. The experiment is performed on 9 tablets of different manufacturers in their normal operating condition. Obtained results detected high ranges of magnetic field in some areas of the tablet surface. This is very important for both manufacturers and users for a safer conduct with tablet computers.*

**Keywords:** Clustering, Magnetic field, Measurement, Tablet

1. **Introduction.** In the last years, the Extremely Low Frequency (ELF) magnetic field effects on human health have been studied and some correlation to children cancers, Alzheimer’s disease and miscarriage has been reported [1]. The mechanisms of influence of these fields remain unclear. ELF fields are thought less harmful than higher frequency fields [2]. Still, in these two studies, no attempt is made to categorize ELF emissions based on clustering of the magnetic component values. Tognola et al. [3] propose a clustering mechanism for estimating the common patterns of children’s exposure to the ELF magnetic field generated by high-voltage sources, such as electric over-lines and others. The focus of their study is limited to high power devices, e.g., heaters but not to low-power electronic devices. Furthermore, Tognola et al. [4] extend their study to include the distances to the emitting source and try to find correlation to the development of leukemia. Indoor devices are not considered in this case. Kozirowska et al. [5] find the effect of the ELF magnetic field on certain chemical components of the honeybee. Using Fourier

spectrum analysis in the infrared range and working with a source of only 50 Hz for more than 2 hours and intensities of  $1.6 \mu\text{T}$ , changes in DNA, RNA and other components occur. A geospatial partitioning of the field distribution in the case of ultra-high frequency magnetic field is proved useful into building non-cummulative and cummulative models to establish the link to the amyotrophic lateral sclerosis [6]. The method may be useful for the study of the ELF magnetic field as well. The harmful effect of the ELF component on infants is being studied in [7]. No attempt is made to classify the different values of the magnetic component but only a 50 Hz emission of  $500 \mu\text{T}$  is considered. Significantly lower dosages of  $28.67 \mu\text{T}$  and less were observed by Abarghooe et al. [8] while creating a multivariate linear regression model revealing the connection to job stress in workers from combined cycle plants. Three groups of emissions are considered depending on the magnetic induction value, but a more flexible division into a higher number of sub-ranges could be employed. Another study [9] of the influence of the ELF magnetic field on humans, occupying commercial areas, relies on the spatial variability of the magnetic level but in the virtually all tested cases the generated maximum is below  $2 \mu\text{T}$ . Appliances, such as F1 freezer, are the primary focus of this study. Duncan et al. [10] look at the ELF emission as a mean to detect and classify electronic activity. They use frequencies between 1 and 1000 Hz and positive results are reported at the use of linear regression analysis, T-distributed stochastic neighbor embedding, dendrogram and Density-Based Spatial Clustering of Applications with Noise (DBSCAN) clustering. Yet, more clustering techniques could be tried. Dehaghi et al. [11] investigate the health effects which the magnetic field, generated by office computers, has on their users. The electric component of the electromagnetic field within the range  $0.26\text{-}1.2 \text{ V/m}$  for desktops and  $0.28\text{-}0.87 \text{ V/m}$  for laptops was the primary object of investigation. It could be extended for the magnetic component as well. The magnetic component distribution is analyzed in [12] with regard to a public access space. Mostly underground and overhead power lines are the sources of an induction with levels from 1 to  $100 \mu\text{T}$ . No attempt is made for clustering of the registered values. Overhead transmission lines are object of investigation in [13], where Luqman et al. propose a plan for proper magnetic field measurement. It is split to path and spot measurement, followed by time management and at the end registering of the actual field values. For the particular experimental configuration, they are between 1 and  $4 \mu\text{T}$ , and the two measurement techniques are alternatively changed among preliminary selected zones based on their suitability. Yet, there is no grouping of the measured values for a further classification. A mapping of static magnetic fields emitted in the vicinity of mobile phones is performed by Zastko et al. [14]. Direct measurements act as mean for building a model by extrapolation down to the size of the phone's screen, and then projecting the resulting values over a 3D model of the head. The magnetic induction values are in the range between  $\mu\text{T}$  and  $\text{mT}$ . The authors do not consider the ELF and radiofrequency fields in the current study, but propose a similar method of measurement for them in order to get a combined field model for assessing the hazards to the human body. An artificial neural network is used in [15] in order to classify the levels of ELF magnetic field generated by high-voltage power lines. These predictions are used to create a 3D map based on latitude and longitude in space of the investigated fields, and find dangerous zones to the human health.

Following the good practices for measuring and classification of the ELF magnetic fields, in our recent studies we managed to successfully classify the level of magnetic induction emitted by laptops [16]. Introducing a partition zone over the surface of the laptop and defining control points for measurement, it is easy to create a map of the emissions [17]. A distinction between normal and stress operating modes of the laptops reveals different dynamic ranges of the ELF magnetic field [18], which is important in the process of deriving recommendations for a safer use during prolonged periods of working. Various clustering techniques [19] proved useful into partitioning the registered values of the ELF

induction to limited numbers of levels, from very low to very high, which eases the process of evaluation of the safety of the laptops. The artificial neural network [20] is another tool that later provides us with the capability of predicting the degree of danger from the ELF emissions sent to the input for classification.

The main goal of this study is to extend our previous analysis of the ELF magnetic field emitted by laptop computers to the tablet computers. Accordingly, we evaluate the efficacy of numerous clustering techniques of the ELF magnetic field values emitted by tablets and measured through suitable partitioning of their top and bottom surface to measuring points.

The rest of the paper is organized as follows. In Section 2, we propose a general methodology for measuring the ELF magnetic field values on tablet devices. In Section 3, we describe various approaches for clustering the magnetic field values. In Section 4, we present experimental results with their analysis and comparison of the tested methods. Finally, in Section 5, we draw a conclusion and outline future work directions.

**2. Measuring the Magnetic Field Levels on Tablet Devices.** The inner components of a tablet working in normal operating condition are fed by a current  $I$  which, flowing through these electronic or electric components, induces a magnetic field  $\mathbf{B}$ . It is composed of its magnitude and direction, and is computed as

$$\mathbf{B}(\mathbf{r}) = B_x \cdot \mathbf{x} + B_y \cdot \mathbf{y} + B_z \cdot \mathbf{z} \tag{1}$$

where  $\mathbf{x}$ ,  $\mathbf{y}$  and  $\mathbf{z}$  are positional vectors orthogonal to each other,  $B_x$ ,  $B_y$  and  $B_z$  are the scalar intensity values of the magnetic induction in the direction of these vectors, respectively, and  $\mathbf{r}$  is radius vector. Starting from these values, the Root Mean Square (RMS) of the magnetic induction  $\mathbf{B}$  can be computed as

$$B = \sqrt{B_x^2 + B_y^2 + B_z^2} \tag{2}$$

We measured the ELF magnetic field through the following devices: (i) Lutron 3D EMF-828 and (ii) Aaronia Spectran NF-5030. Lutron 3D EMF-828 tester with external probe measures the level of the magnetic field at the direction of all three axes ( $X$ ,  $Y$ ,  $Z$  directions), i.e.,  $B_x$ ,  $B_y$  and  $B_z$  in the ELF frequency interval between 30 and 300 Hz. The magnetic field can be measured in three measurement intervals: 20  $\mu\text{T}$ , 200  $\mu\text{T}$  and 2000  $\mu\text{T}$  with a resolution of 0.01  $\mu\text{T}$ , 0.1  $\mu\text{T}$  and 1  $\mu\text{T}$ , respectively. Also, SPECTRAN NF Spectrum Analyzer NF-5030 measures the values of minimum, maximum, average and RMS of the magnetic field at the direction of all three axes, i.e.,  $B_x$ ,  $B_y$  and  $B_z$ , or the total one  $\mathbf{B}$  in the ELF interval between 1 Hz and 1 MHz. The measurement interval goes from 1 pT to 2 mT.

We performed an experiment which consists in measuring the ELF magnetic field at the top and bottom surface of the tablet in 9 different points each (a total of 18 measuring points). It corresponds to the measurement methodology introduced in [16, 18], overcoming the limitations of the TCO standard in measuring the ELF magnetic field emitted by laptop computers. Figure 1 shows the tablet’s top and bottom measuring points.

We examined 9 tablets (named as Tablet 1, . . . , 9) designed by different manufacturers. With the only exception for Tablet 1 which is a convertible with external keyboard,

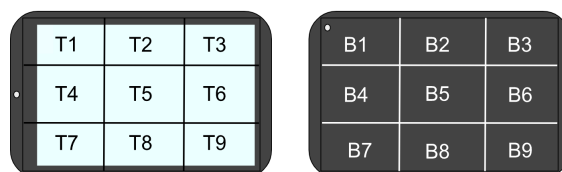


FIGURE 1. Tablet’s top (T) and bottom (B) measuring points

Tablets 2, . . . , 9 do not have external keyboard. In the experiment, we did not consider the keyboard of Tablet 1, because it emits a negligible magnetic field.

All tablets were commonly used in normal operating condition. It means that they work for operating over the Internet or for making Skype calls, viewing pictures, reading documents and for typing. Also, tablets were battery powered only. Figure 2 shows the value of the measured ELF magnetic field at each measuring point (measurement geometry) of the top and bottom parts of the 9 tablets.

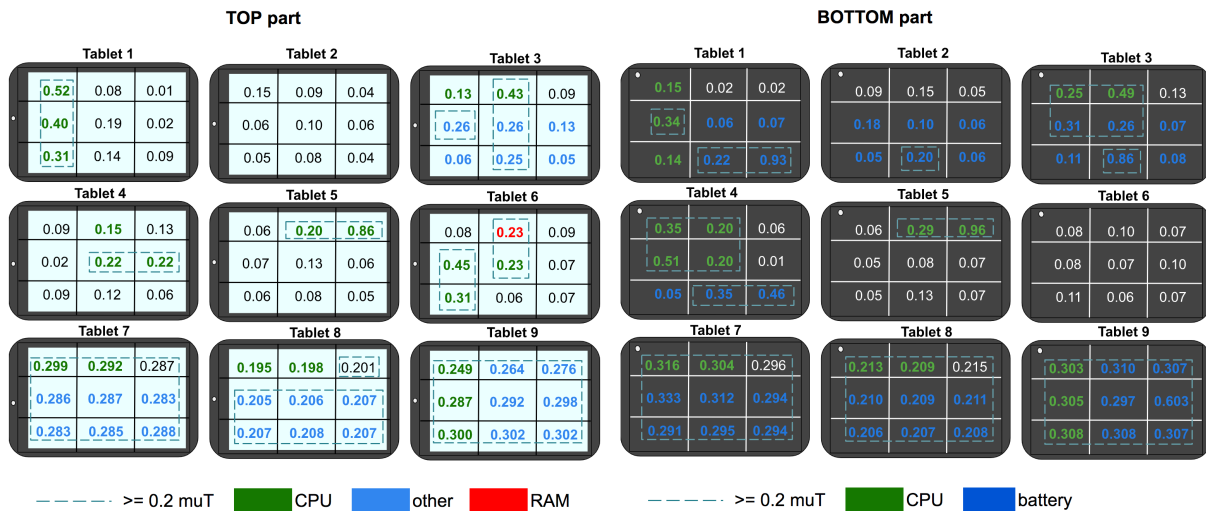


FIGURE 2. (color online) Measured ELF magnetic field at the top and bottom parts of the 9 tablets

It is worth noting that the top part of most tablets emits an ELF magnetic field exceeding  $0.2 \mu\text{T}$ , which is the safety reference limit [16, 18]. In particular, the measured ELF magnetic field in the risk areas ranges between  $0.2 \mu\text{T}$  (Tablets 5, 8) and  $0.86 \mu\text{T}$  (Tablet 5). We can observe that high-risk areas at the top part correspond in most cases to points where CPU (green) and other motherboard components (cyan) are located. Also in the bottom part, most tablets emit an ELF magnetic field exceeding  $0.2 \mu\text{T}$ . In particular, the measured ELF magnetic field in the risk areas ranges between  $0.2 \mu\text{T}$  (Tablets 2, 4, 8) and  $0.93 \mu\text{T}$  (Tablet 1). We can observe that high-risk areas at the bottom part correspond in most cases to points where CPU (green) and battery (blue) are located.

**3. Approaches for Clustering the Magnetic Field Levels.** We stored the ELF magnetic field measured at the 9 top and 9 bottom points of the 9 tablets in two datasets with 81 values each. Accordingly, the top (resp. bottom) dataset collects the RMS values of the measured ELF magnetic field induction  $B$  at the top (resp. bottom) surface of the tablets. The aim is to detect the danger levels of exposure to ELF magnetic field emitted by tablet computers in the normal operating condition. To pursue this goal, we apply and compare different clustering methods for each dataset, in order to detect ELF magnetic field ranges at the top and bottom parts of the tablet. In particular, we use four clustering methods for binning one-dimensional data: (i) partitional, (ii) model-based, (iii) hierarchical, and (iv) density-based.

**3.1. Partitional clustering.** We selected three partitional clustering algorithms: (i) K-means, (ii) K-medians, and (iii) Fuzzy C-means.

In K-means algorithm [21, 22], the input parameter  $K$  for the clusters (ranges) is predetermined. The centroid of each cluster, which is the mean of its data points, serves as the foundation for the algorithm. The process begins by choosing  $K$  initial centroids

at random and assigning each data point to its nearest centroid using the Euclidian distance. The second step involves recalculating the new  $K$  centroids using the previous assignments. The centroids move about gradually as these two procedures are repeated until no more adjustments are needed.

Also, K-medians algorithm [23, 24] consists of analogous phases of the K-means algorithm. The main differences are (i) the cluster's centroid is calculated as the median value of the data points that make up the cluster, and (ii) the Manhattan distance is used to compute the distance between data points and centroids. K-medians produces more compact clusters than K-Means and provides robustness to outliers.

Finally, in Fuzzy C-means [25], the input data points used in the clustering procedure may be a component of multiple clusters. The following objective function's minimization must be given for convergence to take place:  $J = \sum_{i=1}^D \sum_{j=1}^K \lambda_{ij}^m \|x_i - c_j\|^2$ , where  $D$  is the number of data points,  $K$  the number of clusters,  $m$  a factor influencing the fuzzy overlap represented by a real number greater than 1,  $x_i$  the  $i$ -th data point,  $c_j$  the center of the  $j$ -th cluster, and  $\lambda_{ij}$  the level of belonging of  $x_i$  to the  $j$ -th cluster.

**3.2. Model-based clustering.** We adopted two model-based clustering algorithms: (i) Self-Organizing Map, (ii) Expectation-Maximization with Gaussian Mixture Models.

Kohonen's Self-Organizing Map (SOM) [26, 27] is built on a neural network that learns to predict the output based on the "shape" of the training data. An algorithm made up of several stages is iteratively run to train the network, beginning with the first epoch.

Without the availability of a direct solution, the Expectation-Maximization (EM) algorithm [28] is used to statistical models for the estimation of maximum likelihood parameters. The input often contains latent variables and unknown parameters together with partial data observations. With the likelihood function, the derivatives of all unknown values, latent variables, and parameters could be used to find a maximum as a solution.

**3.3. Hierarchical and density-based clustering.** Agglomerative hierarchical clustering [29] is a bottom-up method that merges pairs of clusters by starting at the lowest level of the hierarchy and working up. A dendrogram is a common visual representation of the resulting hierarchy. A measure of dissimilarity between the input data points is used to determine whether two clusters should be combined.

About density-based clustering, DBSCAN [30] is a method that identifies high density areas and the low density areas that lie between them. The density is defined as the number of points covered by a given radius ( $Eps$ ). Three types of points are being introduced for the purposes of analysis: (i) core points, such that their number ( $MinPts$ ) is over a certain number within  $Eps$  so they form the cluster itself, (ii) border points, which are fewer than  $MinPts$  encapsulated by  $Eps$  and still are in the neighbourhood of the core points, and (iii) noise points, which are all the other points from the dataset.  $N$  data points are provided as input together with the globally determined  $Eps$  and  $MinPts$ .

**4. Comparison of Methods and Results.** We compare the ELF magnetic field ranges detected by the aforementioned algorithms for the tablets' top ranges (Figure 3) and bottom ranges (Figure 4). Considering the top ranges, hierarchical clustering and K-means clustering detected a higher minimum ELF magnetic field than the other approaches, especially for the "very high" cluster (Figure 3, left). Similar can be observed for the maximum values; however, in this case all the used algorithms have detected the same maximum value of ELF magnetic field for the cluster "very high" (Figure 3, right). For the tablet's bottom, the detected minimum value was higher when using DBSCAN and hierarchical clustering for "very low", "low", "middle" and "high" clusters, but for the "very high" cluster K-means and Fuzzy C-means also detected high minimum values in addition to DBSCAN and hierarchical clustering. For the maximum values, DBSCAN also has the tendency to detect higher maximum values in each class. It is interesting to

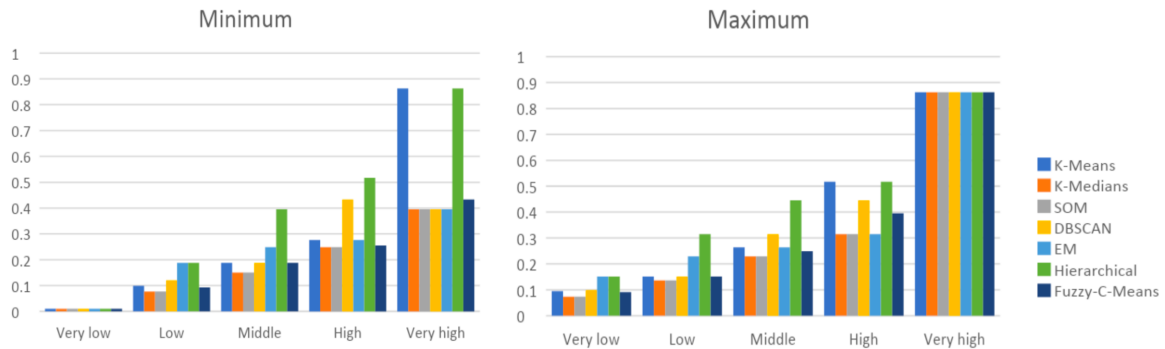


FIGURE 3. (color online) Top range minimum and maximum ELF magnetic field

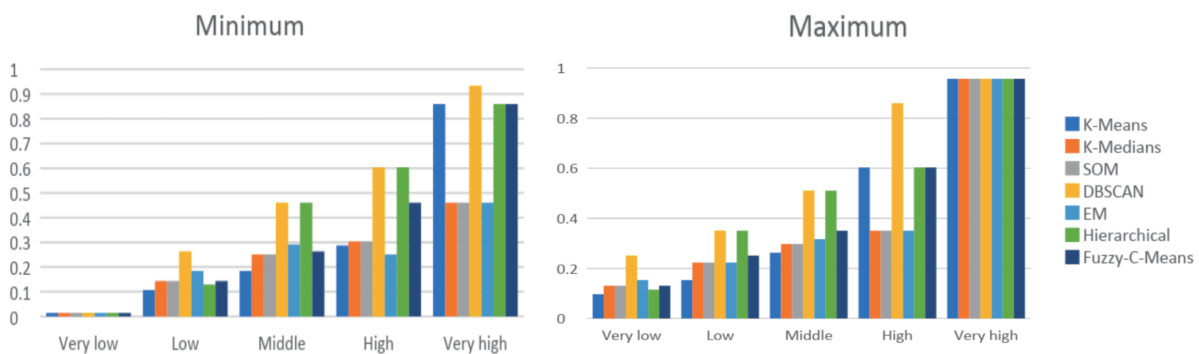


FIGURE 4. (color online) Bottom range minimum and maximum ELF magnetic field

observe that in the “high” cluster, higher maximum values were detected by the K-means, hierarchical clustering, Fuzzy C-means and DBSCAN, while for the “very high” class all the algorithms detected the same maximum value.

In addition, a minimum difference is observed between the top and bottom ranges. However, the minimum and maximum values of the ELF magnetic field are higher at the bottom part of the tablet compared to the top part. Middle, high, and very high ranges all have values of the ELF magnetic field above the reference limit of  $0.2 \mu\text{T}$ , with the middle range representing the borderline as its minimum values are just slightly below the reference limit at the top part. As for the very low and low ranges, they are generally considered safe as their detected maximum values on the top of the tablet do not cross the reference limit except for hierarchical clustering and EM clustering. However, for the bottom part of the tablet the low emission range exhibits minimum values higher than the reference limit when using the DBSCAN clustering approach, while all clustering approaches except K-means detected maximum values higher than the reference limit.

We can observe that K-medians algorithm is the best choice for detecting the danger classes, because K-means, SOM and agglomerative hierarchical clustering approaches detected ranges that might be made of single values, and the differences between top and bottom ranges are not clearly detected. In addition, the DBSCAN algorithm is prone to detecting very large ranges, as seen in Figures 3 and 4, while the EM algorithm detected overlapping ranges. Both the K-medians and Fuzzy C-means showed good performance as these algorithms did not detect overlapping ranges; however, the K-medians is a much better approach for detecting the ELF magnetic field ranges emitted by tablets as it differentiates between the top and bottom emissions better.

Accordingly, Figure 5 shows the top and bottom danger maps of exposure to ELF magnetic field obtained by the K-medians clustering. The top (resp. bottom) map associates

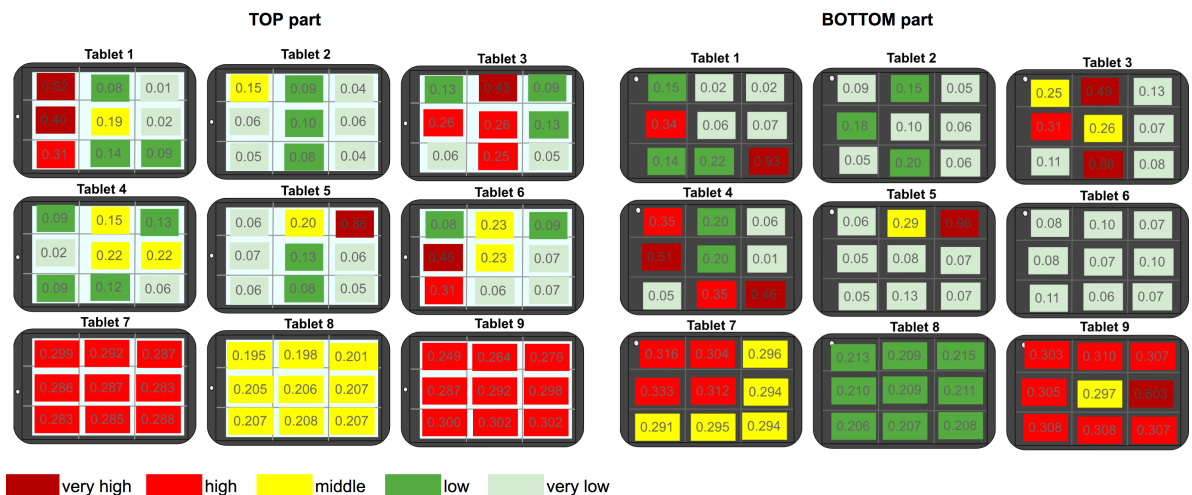


FIGURE 5. (color online) Top and bottom danger maps obtained by the K-medians algorithm

each measuring top (resp. bottom) point to the corresponding ELF magnetic field range according to its value. Here, we can observe that a very high range of ELF magnetic field emissions is located at the CPU area (Figure 2, Figure 5 Tablets 1, 3, 5, 6 (top) and Tablets 3, 4, 5 (bottom)), as well as at the battery area (Figure 2, Figure 5 Tablets 1, 3, 4, 9 (bottom)), while the middle levels are emitted by the RAM (Figure 2, Figure 5 Tablet 6 (top)). Other motherboard components were found to emit very low to high emissions, depending on the tablet (Figure 2, Figure 5 Tablets 3, 7, 8, 9 (top)).

**5. Conclusions.** In this paper, we introduced a new method for measuring the ELF magnetic field ranges emitted by tablet computers using clustering methods. In particular, we compared partition-based, model-based, hierarchical and density-based clustering approaches. We tested the proposed method on 9 tablets. First, we measured the ELF magnetic field emissions at the top and bottom parts of their surface in normal operating condition. Then, we employed clustering on the top and bottom measured values for detecting the ELF magnetic field ranges. In the end, we realized that K-medians algorithm is more robust than the other algorithms in detecting ELF magnetic field ranges emitted by tablets. The proposed method can be very helpful in identifying the risk levels of exposure to magnetic fields from the tablet users. Also, from the danger maps, it is possible to explore the most dangerous tablet’s inner components in terms of ELF magnetic field level. It will hopefully provide useful information to the manufacturers, for a more careful production of the inner components, and to the tablet users, for a more cautious use of the device. In particular, we suggest to avoid to directly keep in touch with the tablet device, using the mouse and external keyboard. In the future, we will explore the tablet under the so called “stress condition”, i.e., when it is overloaded with heavy programs.

**Acknowledgment.** This work is partially supported by the Ministry of Education, Science and Technological Development of the Republic of Serbia through the Mathematical Institute of the Serbian Academy of Sciences and Arts, Serbia. This work is dedicated to the memory of Prof. Darko Brodić with full gratitude.

**REFERENCES**

[1] A. Karimi, F. G. Moghaddam and M. Valipour, Insights in the biology of extremely low-frequency magnetic fields exposure on human health, *Molecular Biology Reports*, vol.47, no.7, pp.5621-5633, 2020.

- [2] T. Miah and D. Kamat, Current understanding of the health effects of electromagnetic fields, *Pediatric Annals*, vol.46, no.4, pp.172-174, 2017.
- [3] G. Tognola, E. Chiaramello, M. Bonato, I. Magne, M. Souques, S. Fiocchi, M. Parazzini and P. Ravazzani, Cluster analysis of residential personal exposure to ELF magnetic field in children: Effect of environmental variables, *International J. Environmental Research and Public Health*, vol.16, no.22, 4363, 2019.
- [4] G. Tognola, M. Bonato, E. Chiaramello, S. Fiocchi, I. Magne, M. Souques, M. Parazzini and P. Ravazzani, Use of machine learning in the analysis of indoor ELF MF exposure in children, *International J. Environmental Research and Public Health*, vol.16, no.7, 1230, 2019.
- [5] A. Koziorowska, J. Depciuch, J. Bialek, I. Wos, K. Koziol, S. Sadlo and B. Piechowicz, Electromagnetic field of extremely low frequency has an impact on selected chemical components of the honeybee, *Polish J. Veterinary Sciences*, vol.23, no.4, pp.537-544, 2020.
- [6] J. Luna, J. P. Leleu, P. M. Preux, P. Corcia, P. Couratier, B. Marin, F. Boumediene and F. Consortium, Residential exposure to ultra high frequency electromagnetic fields emitted by Global System for Mobile (GSM) antennas and amyotrophic lateral sclerosis incidence: A geo-epidemiological population-based study, *Environmental Research*, vol.176, 108525, 2019.
- [7] H. Ozturk, D. Saribal, Y. M. Gelmez, G. Deniz, A. Yilmaz, A. Kirectepe and A. M. Ercan, Extremely low frequency electromagnetic fields exposure during the prenatal and postnatal periods alters pro-inflammatory cytokines levels by gender, *Electromagnetic Biology and Medicine*, vol.41, no.2, pp.163-173, 2022.
- [8] S. E. Abarghooe, G. H. Halvani, F. Kargar-Shouroki, H. Mihanpour and F. Madadizadeh, Job stress among workers exposed to extremely low frequency electric and magnetic fields in a combined cycle power plant, *J. Environmental Health and Sustainable Development*, vol.7, no.2, pp.1614-1622, 2022.
- [9] I. Pavel, V. David and S. Ursache, On a survey of the magnetic field in a commercial area, *Proc. of the 22nd IMEKO TC4 International Symposium & 20th International Workshop on ADC Modelling and Testing Supporting World Development through Electrical & Electronic Measurements*, Iasi, Romania, pp.300-304, 2017.
- [10] C. Duncan, O. Gkountouna and R. Mahabir, Theoretical applications of magnetic fields at tremendously low frequency in remote sensing and electronic activity classification, *Advances in Computer Vision and Computational Biology*, pp.235-247, 2021.
- [11] B. F. Dehaghi, A. Ghamar, L. I. Ghavamabadi and S. M. Latifi, Health effects of exposure to electromagnetic fields generated by computers in a Government Office in Ahvaz City-2016, *Journal of Health in the Field*, vol.5, no.2, 2017.
- [12] G. Roşu and O. Baltag, The analysis of magnetic field measurements in a public access area, annals of the University of Craiova, *Electrical Engineering Series*, no.40, pp.135-140, 2016.
- [13] H. M. Luqman, M. N. R. Baharom, H. Ahmad and I. Ullah, Planning and conducting magnetic field level measurement from overhead transmission line, *International Journal of Electrical and Computer Engineering*, vol.7, no.6, 3124, 2017.
- [14] L. Zastko, L. Makinistian, A. Tvarožná, F. L. Ferreyra and I. Belyaev, Mapping of static magnetic fields near the surface of mobile phones, *Scientific Reports*, vol.11, no.1, pp.1-10, 2021.
- [15] F. H. Sakacı and O. Cerezci, Prediction of magnetic pollution with artificial neural network in living areas, *Journal of Electrical Engineering & Technology*, vol.16, no.5, pp.2701-2708, 2021.
- [16] D. Brodić and A. Amelio, Classification of the extremely low frequency magnetic field radiation measurement from the laptop computers, *Measurement Science Review*, vol.15, no.4, pp.202-209, 2015.
- [17] D. Brodić, Measurement of the extremely low frequency magnetic field in the laptop neighborhood, *Revista Facultad de Ingeniera Universidad de Antioquia*, no.76, pp.39-45, 2015.
- [18] D. Brodić and A. Amelio, Detecting of the extremely low frequency magnetic field ranges for laptop in normal operating condition or under stress, *Measurement*, vol.91, pp.318-341, 2016.
- [19] D. Brodić and A. Amelio, Time evolving clustering of the low-frequency magnetic field radiation emitted from laptop computers, *Measurement*, vol.99, pp.171-184, 2017.
- [20] D. Brodić, D. Tanikić and A. Amelio, An approach to evaluation of the extremely low-frequency magnetic field radiation in the laptop computer neighborhood by artificial neural networks, *Neural Computing and Applications*, vol.28, no.11, pp.3441-3453, 2017.
- [21] A. Gupta, K. G. Mehrotra and C. Mohan, A clustering-based discretization for supervised learning, *Statistics & Probability Letters*, vol.80, nos.9-10, pp.816-824, 2010.
- [22] J. MacQueen, Some methods for classification and analysis of multivariate observations, *The 5th Berkeley Symposium on Mathematical Statistics and Probability*, CA, USA, pp.281-297, 1967.
- [23] P. S. Bradley, O. L. Mangasarian and W. N. Street, Clustering via concave minimization, *Advances in Neural Information Processing Systems*, vol.9, pp.368-374, 1997.



- [24] H. Wang and J. Zhang, One-dimensional  $k$ -center on uncertain data, *Theoretical Computer Science*, vol.602, pp.114-124, 2015.
- [25] J. C. Bezdek, *Pattern Recognition with Fuzzy Objective Function Algorithms*, Plenum Press, New York, 1981.
- [26] T. Kohonen, Self-organized formation of topologically correct feature maps, *Biological Cybernetics*, vol.43, no.1, pp.59-69, 1982.
- [27] M. Vannucci and V. Colla, Meaningful discretization of continuous features for association rules mining by means of a SOM, *European Symposium on Artificial Neural Networks*, Bruges, Belgium, pp.489-494, 2004.
- [28] A. P. Dempster, N. M. Laird and D. B. Rubin, Maximum likelihood from incomplete data via the EM algorithm, *J. Royal Statistical Society Series B*, vol.39, no.1, pp.1-38, 1977.
- [29] L. Rokach and O. Maimon, *Clustering Methods, Data Mining and Knowledge Discovery Handbook*, Springer, US, 2005.
- [30] M. Ester, H. Kriegel, J. Sander and X. Xu, A density-based algorithm for discovering clusters in large spatial databases with noise, *The 2nd International Conference on Knowledge Discovery and Data Mining*, Portland, OR, pp.226-231, 1996.